ROCK SLOPE ASSESSMENT USING KINEMATIC AND FINITE ELEMENT ANALYSIS: AN EXAMPLE FROM MALEKHU-DHADINGBESHI SECTION OF NH43, CENTRAL NEPAL

Nirmal Kafle¹*, Raju Miyan ¹, Aanand Kumar Mishra ¹

¹Department of Civil Engineering, Khwopa College of Engineering, Tribhuvan University, Nepal

Abstract

Slope stability in the Himalayas is a critical issue due to the region's unique geological and tectonic characteristics. The rocks of Himalayas are fragile and weak due to complex deformational structures causing the instability of slopes which are common, posing significant risks to infrastructure and communities. The central Nepal is characterized by similar problems and while constructing the engineering structures, challenges might be encountered. This study is aimed at modelling slope stability along the Malekhu-Dhadingbeshi road section of NH43 lying at the central Nepal lesser Himalaya using Kinematic analysis and Finite Element Method (FEM) modelling. The FEM modelling was conducted using two different computer programs. It was carried out at six different potential slopes with multifaceted geometry composed of slightly to moderately weathered quartzites and phyllites. The potential slope sections were identified using satellite imagery and field observations with key indicators including the condition of the slope toe, the presence of dislodged rocks and the formation of tension cracks. Their geometries were then created from the survey data obtained from topographic survey in the field. Input parameters for the modeling, such as cohesion and friction angle were calculated using the Hoek-Brown criterion while unit weight, elastic modulus and uniaxial compressive strength of rocks were determined from laboratory tests. The modelling was carried out under static condition provided there are no external influences from seismic activity or water forces. Out of six identified slopes sections, three of them were found to be critical during kinematic analysis, which were further modelled using FEM. Results from FEM revealed the non-significant total displacement at all of the three slope sections with higher critical Strength Reduction Factor (SRF) making the slopes stable. The findings also highlight the strength of the slopes under current conditions, providing valuable information for infrastructure planning in the region.

Keywords: Slope stability, Kinematic analysis, Finite element method, Strength reduction factor

1. Introduction

The stability of rock slopes is a fundamental concern in engineering geology and infrastructure development, particularly in mountainous regions. Slope failures are becoming increasingly widespread all over the world due to changes in climate conditions and anthropogenic causes that aggravate landslide incidence (Fidan et al., 2024). Unstable slopes often experience surficial movement or inter-

*Corresponding author: Nirmal Kafle Khwopa College of Engineering, Bhaktapur Email: nirmalkafle1917@gmail.com (Received: Jan. 5, 2025, Accepted: April 11, 2025) https://doi.org/10.3126/jsce.v12i1.78365 nal deformation, leading to the release of loose rock blocks along weak geostructural features (Rechberger et al., 2021). Rock slope morphologies are primarily influenced by penetrative discontinuities like bedding planes and are continuously shaped by various failure modes, depending on the arrangement of these discontinuities relative to the slope (Cruden and Hu, 1993). Consequently, the analysis and modeling of slope stability is absolutely essential for the safe and reliable design and construction of infrastructure in landslide-prone regions (Habtamu et al., 2022). A wide range of conventional and numerical modeling methods have been employed globally to evaluate slope stability in diverse geological and geotechnical settings. The kinematic

approach is commonly employed to assess the failure mode of rock slopes along specific planes (e.g., joints, faults, and shear zones), without considering the forces responsible for the failure (de Freitas, 2009). If the kinematic analysis indicates that a rock slope is unstable, then the kinetic stability of the rock slope is assessed using the numerical analysis method (Park et al., 2016). The FEM represents a powerful alternative approach for slope stability analysis which is accurate, versatile and requires fewer a priori assumptions, especially, regarding the failure mechanism. It is argued that the FEM of slope stability analysis is a more powerful alternative to traditional limit equilibrium method and its widespread use should now be standard in geotechnical practice (Griffiths and Fenton, 2004) This study integrates kinematic and numerical analyses to evaluate the stability of selected slopes along the Malekhu-Dhadingbesi section of National Highway- NH43 (DoR, 2021). The study area was chosen due to its critical importance as a vital transportation link in the region, coupled with the inherent geological and tectonic challenges posed by the Himalayan terrain. Consequently, this study aims to model the vulnerable slope sections along the road. To achieve this, Kinematic analysis and continuum modeling using the FEM approach was employed, as it is particularly well-suited to the area's geology, characterized by relatively uniform geotechnical properties.

2. Geology of the Study Area

The study area is located in central Nepal, within the Lesser Himalayan region (Figure 1). The specific formations examined in this study include the Lower and Upper Nawakot Groups of the Nawakot Complex. The formations of these groups extend roughly northwest to southeast, generally dipping southward, and are part of the northern limb of the Mahabharat Synclinorium (Stöcklin, 1980). Moreover, the critical slope sections that have been identified primarily consist quartzites and phyllites. The quartzite unit is outcropped in the study area, forming steep ridges. Its properties are primarily influenced by open, moderately to steeply sloping, tightly spaced persistent systematic joint sets. The phyllite is mostly exposed in the study area at an interface between quartzites. The region's tectonic activity has resulted in numerous discontinuities, which significantly influence slope stability.

3. Methodology

During the current study, Kinematic analysis was carried out and FEM technique was deployed to model the slope stability in the study area. To ascertain the stability of the slope, these methods mainly employ characteristics like slope geometry, unit weight, Poisson ratio, Young's modulus, and shear strength parameters. This study used a comprehensive data-gathering procedure and stability modeling

techniques.

3.1. Data Collection

A comprehensive field survey was carried out across the study area to identify critical slope segments, analyze geological characteristics, and collect slope geometry data for slope stability modeling. Critical slope sections were selected based on satellite imagery analysis and field observations. Key indicators included the condition of the slope toe, the presence of dislodged rocks and the formation of tension cracks (Figure 2). Once the critical slope sections were identified, slope profiles and geometries were developed by integrating field measurements with geological and topographical data. The topographical data were collected by conducting topographical survey of the individual slopes using Electromagnetic Distance Measurement (EDM). The geological units comprising these critical slope sections were then analyzed, with certain parameters assessed directly in the field. Discontinuity characteristics, such as aperture, joint wall weathering, orientation, spacing, persistence, infill material, roughness, and groundwater conditions, were evaluated in accordance with the (ISRM, 1979) standards. Additionally, the Uniaxial Compressive Strength (UCS) of intact rocks, an essential parameter for determining shear strength, was measured in situ using the Schmidt hammer (Type N Rebound Hammer) rebound test and verified it with the laboratory tests.

Rock samples were systematically collected from each identified critical slope segment to evaluate their geotechnical properties. The sampling process was carefully designed to ensure adequate representation of the rock types within the slope sections. Laboratory tests were subsequently conducted on these representative samples to determine key parameters, including UCS, elastic modulus as well as unit weight for rocks. The cohesion (c) and friction angle (ϕ) of geological materials are crucial parameters for analyzing slope stability using FEM (Wyllie and Mah, 2017). Accordingly, the cohesion and friction angle of rocks were calculated using rock mass friction angle and cohesion charts (Hoek and Brown, 1997) following generalized Hoek-Brown Failure criteria (Hoek et al., 2002). This criterion uses parameters such as the Geological Strength Index (GSI), UCS of intact rocks, material constant of intact rock (mi), disturbance factor (D), slope height, and unit weight of rocks to determine the abovementioned parameters. In this work, the parameters for this criterion were established in the following ways:

- The Geological Strength Index (GSI) was determined from the equation, GSI = $RMR_{89}-5$ for $RMR_{89}>23$ (Hoek and Kaiser, 1995). The Rock Mass Rating (RMR) was calculated on field.
- ullet The UCS of intact rock σ_{ci} was determined from the laboratory tests.

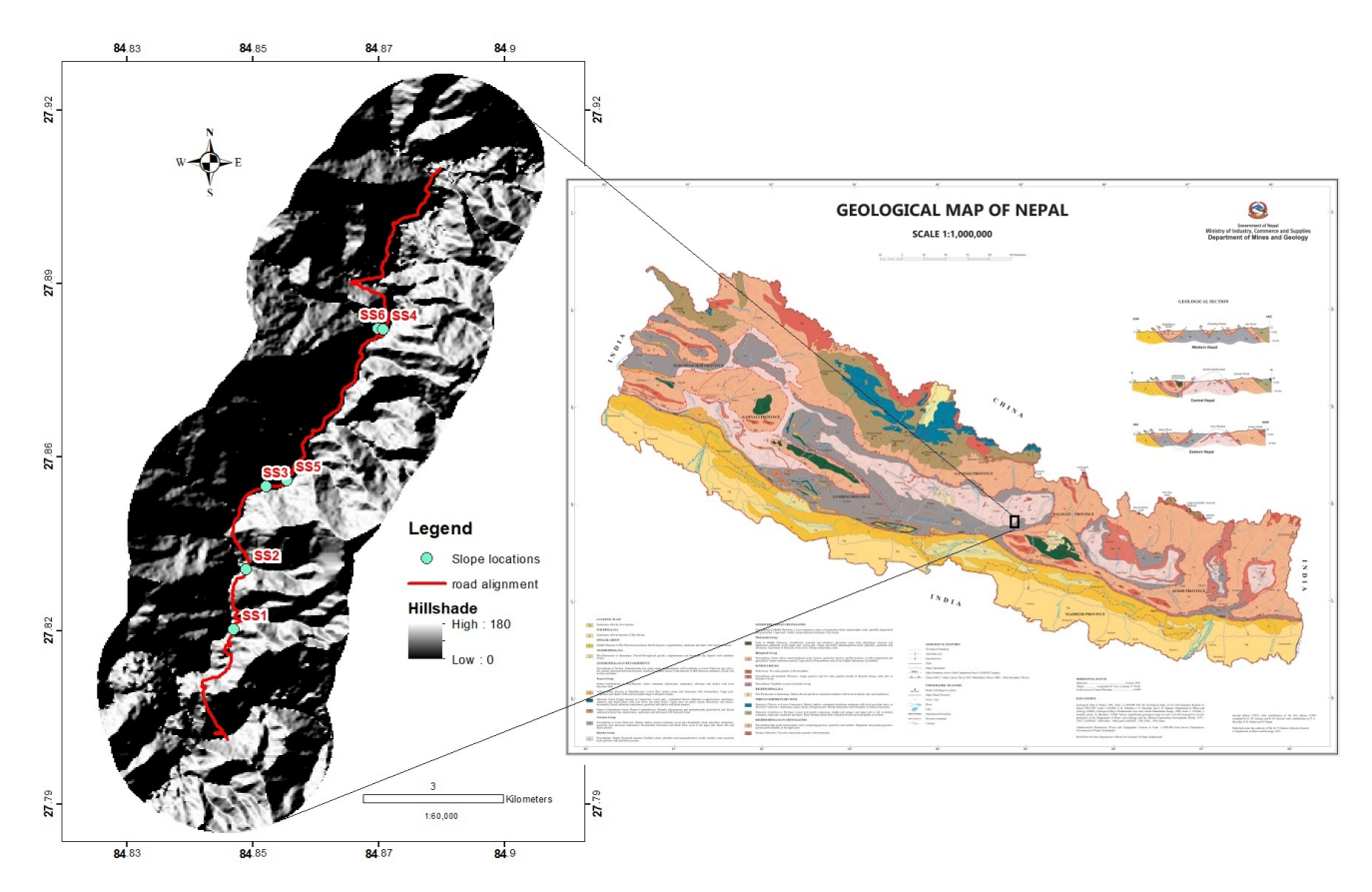


Figure 1. Location map showing the study area with slope sections and road alignment on geological map of Nepal (DMG, 2023)

- The material constant of intact rock (m_i) and rock mass strength parameter (m_b) was adopted from (Hoek and Marinos, 2007).
- The disturbance factor (D) was estimated using the recommendations proposed by (Wyllie and Mah, 2017). Therefore, a disturbance factor of 0.7 was utilized, considering that controlled blasting can result in little rock damage on the slope.
- The unit weight (γ) of the rock was measured in the laboratory, while the height of the slope was determined in the field using a measuring tape.
- Finally, the cohesion (c), friction angle (ϕ), and elastic modulus (E), empirical constants (a and s) were determined using generalized Hoek-Brown Failure criteria.

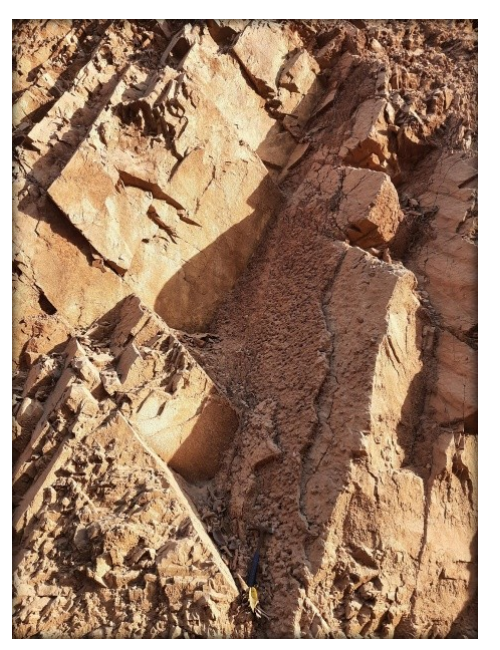
Moreover, for the rock formation, the Poisson ratio (ν) of rocks was determined using Equation (1), forwarded by (Vásárhelyi, 2009) from input parameters such as GSI and intact rock material constant.

$$\nu = 0.002 \times GSI - 0.003 \times m_i + 0.457 \tag{1}$$

3.2. Kinematic Analysis and Numerical Analysis

A total of six sites were selected for detailed investigation based on preliminary field assessments and geological conditions which is presented in Table 1. To evaluate potential slope instabilities, kinematic analysis was performed for each site using stereographic projection. This analysis focused on identifying possible failure mechanisms, including planar, wedge, and toppling failures, by comparing the orientations of discontinuities with the respective slope orientations using Dips 7.0 (Rocscience, 2016).

The critical slopes resulting from the kinematic analysis of six slopes is selected for further numerical analysis to conduct a more comprehensive stability assessment. Numerical analysis was subsequently employed to evaluate the stability and deformation characteristics of critical slopes under static conditions. Numerical analysis involved FEM through the use of Phase2 Version 8.0 (Rocscience, 2015) and PLAXIS 2D CONNECT Edition V20 (Bentley Systems, 2019). Both of the computer program offers distinct features and modeling approaches that cater to different aspects of rock slope engineering. Model configuration was established, including the definition of geometry, boundary





(a) SS3 (b) SS4

Figure 2. Existing field condition

Table 1. Potential slope sections identified during detailed investigation

Slope section	Location		Brief description of identified potential critical slopes sections
	Е	N	
SS1	287775	3079472	Consisting of moderately weathered slate of Benighat Slate
SS2	288373	3082486	Consisting of slightly weathered quartzite of Nourpul Formation
SS3	288896	3082704	Consisting of slightly weathered quartzite of Nourpul Quartzite
SS4	288049	3080749	Consisting of slightly weathered quartzite of Fagfog Quartzite
SS5	290681	3085776	Consisting of moderately weathered phyllite and quartzite of Kuncha Formation
SS6	290790	3085852	Consisting of moderately weathered phyllite and quartzite of Kuncha Formation

conditions, and material properties. The Hoek-Brown failure criterion was applied to characterize material properties. The model boundaries were discretized, and a mesh was generated automatically based on model geometry. Simulations were performed under static conditions, applying the Strength Reduction Method (SRM). SRM technique is often used with FEM to solve sophisticated problems such as estimating stability of slope (Cala and Flisiak, 2020).

4. Results and Discussion

4.1. Kinematic Analysis

Using the Dips 7.0, the kinematic analysis of all the six potential slope sections were carried out (Figure 3). The kinematic analysis revealed that wedge and planar failures are the predominant failure modes in the study area. Out of the six slope sections under analysis, three slope sections

SS2, SS3, and SS4 demonstrate characteristics that suggest a risk of instability or potential failure (Figure 3b, 3c and 3d.). This could be due to factors such as unfavorable joint orientations, steep dip angles, or low friction angles along discontinuities, which align with conditions that promote sliding or toppling. These sections meet the criteria for kinematically admissible failure, where the dip of the potential failure plane exceeds the internal friction angle but remains below the slope face angle. In contrast, the remaining three slope sections SS1, SS5, and SS6 appear stable (Figure 3a, 3e and 3f.). This suggests that the geological conditions in these areas are less conducive to failure. Possible reasons for their stability could include more favorable joint orientations, lower dip angles, higher friction angles, or the absence of intersecting discontinuities that could lead to block movement. Essentially, the structural configurations in these sections do not support the formation of potential failure planes, indicating that the slopes are unlikely to experience significant displacement or failure under normal conditions. Several additional parameters such as shear strength of discontinuities, groundwater pressure and seismic impacts may influence the stability of the analyzed slope which has not been considered in this study. Since three slopes SS2, SS3 and SS4 among six studied slopes are found critical from kinematic analysis, the results of the same slopes has only been presented.

Table 2 summarizes the kinematic analysis result of SS2 which suggest that out of all analyzed discontinuities planar sliding is the most common failure mode (45.00%) followed closely by wedge sliding (41.38%). Direct toppling represents a smaller proportion (15.58%) of potential slope failures. The percentages indicate how dominant each failure mode is within the slope section based on geological data. Higher percentages suggest a greater risk of failure under those conditions. The overall stability of the slope might have been significantly influenced by the high friction angle (38°) and steep dip (65°).

Table 2. Kinematic analysis result SS2

Kinematic Analysis	Planar	Wedge	Direct
	Sliding	Sliding	Toppling
	(All)		
Slope Dip		65°	
Slope Dip Direction		155°	
Friction Angle		38°	
Critical	36	1304	491
Total	80	3151	3151
Total (%)	45.00	41.38	15.58

Table 3 summarizes the kinematic analysis result of SS3 where direct toppling shows the highest number of critical cases (474) with 16.65%, while planar sliding has the high-

est percentage of critical cases (21.05%). Wedge sliding, despite being the most frequent, has the lowest critical percentage (13.21%). This suggest that although planar sliding has fewer critical cases than toppling, it has highest proportion of critical cases relative to total analyzed discontinuities. This means planar sliding are more likely to be critical compared to other failure types.

Table 3. Kinematic analysis result SS3

Kinematic Analysis	Planar	Wedge	Direct
	Sliding	Sliding	Toppling
	(All)		
Slope Dip		70°	
Slope Dip Direction		126°	
Friction Angle		42°	
Critical	16	376	474
Total	76	2846	2846
Total (%)	21.05	13.21	16.65

From Table 4, which shows the kinematic analysis of SS4, wedge sliding has the highest percentage of critical cases (31.94%), making it the dominant failure mode. Planar sliding also shows significant risk (25.00%), while direct toppling represents a lower but notable share (17.89%). The slope's steep dip (75°) and high friction angle (42°) indicate potential stability, but wedge sliding remains a primary concern for mitigation efforts. The kinematic analysis of six slope sections identifies wedge and planar failures as the primary instability mechanisms, with SS2, SS3, and SS4 being particularly susceptible due to unfavorable joint orientations, steep dip angles, and low friction angles. SS2 is prone to planar sliding and wedge sliding, while SS3 shows significant direct toppling, and SS4 is dominated by wedge sliding. In contrast, SS1, SS5, and SS6 remain stable due to favorable structural conditions. The findings align with prior research emphasizing the role of discontinuity orientations and friction angles in slope stability, though external factors like groundwater and seismic activity were not considered.

Table 4. Kinematic analysis result SS4

Kinematic Analysis	Planar	Wedge	Direct
	Sliding	Sliding	Toppling
	(All)		
Slope Dip		75°	
Slope Dip Direction		280°	
Friction Angle		42°	
Critical	60	564	316
Total	15	1766	1766
Total (%)	25.00	31.94	17.89

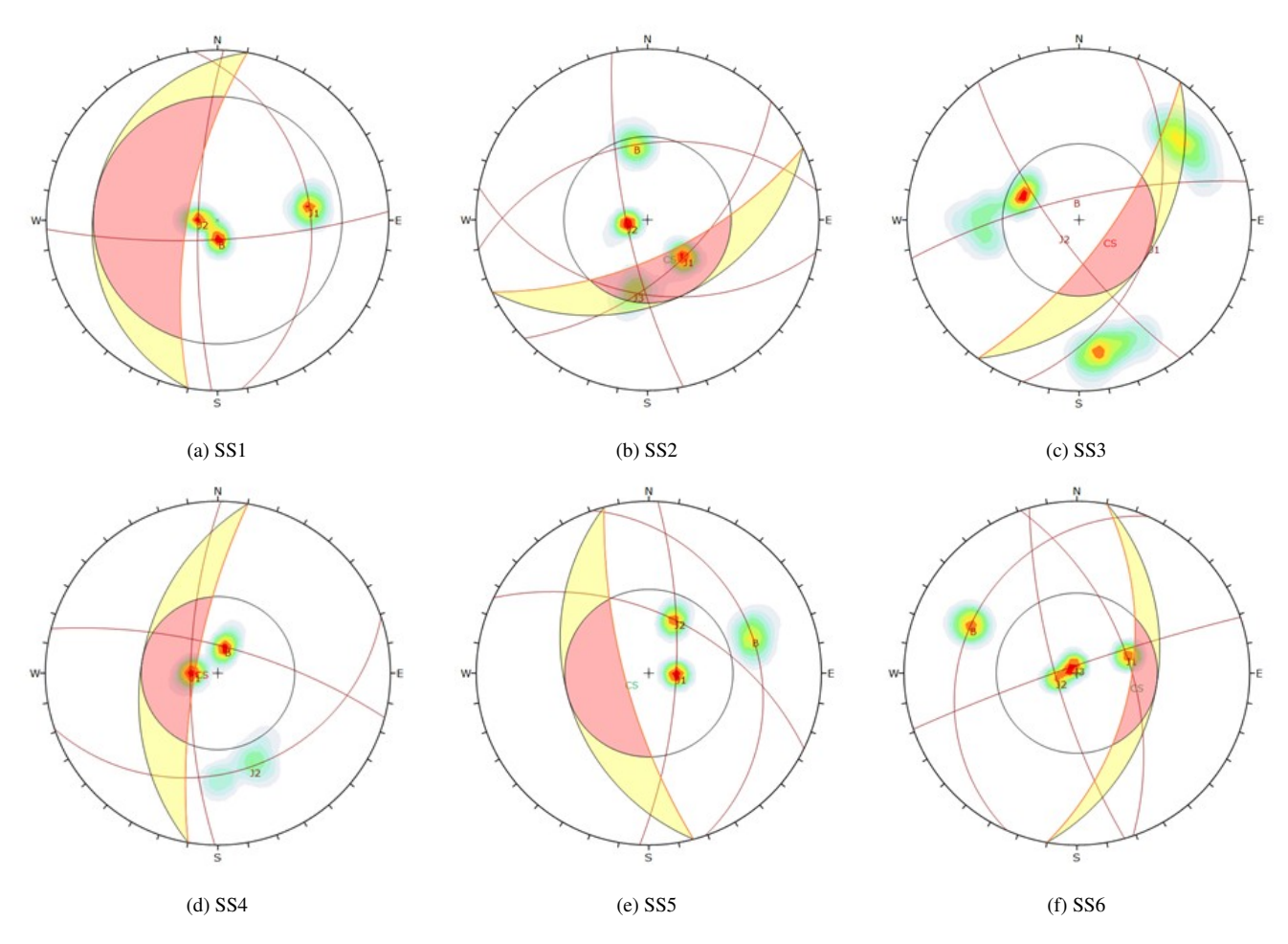


Figure 3. Kinematic analysis of different six slope sections

4.2. FEM Modelling

Finite element modeling was conducted using Phase2 and PLAXIS 2D to assess slope stability under static conditions. Table 5 summarizes the input data for FEM modelling.

Stability modelling using Phase2

Phase2 employs the FEM to simulate stress distribution and deformation within rock slopes. The SRM is commonly integrated into the analysis to estimate the factor of safety (FoS) by gradually reducing the material strength parameters until failure occurs. During this FEM slope modeling, the material properties and slope geometry remained consistent. This modelling revealed that SS2, SS3 and SS4, all of the potential slopes are stable under projected condition under absence of any seismic and water force (Figure 4).

The analysis indicates that the slope structure designated as SS2, SS3 and SS4 demonstrates higher stability under

Table 5. Input data for FEM modelling

Parameter	Unit	Slope Section		
		SS2	SS3	SS4
$\overline{\gamma}$	kN/m ³	22.240	25.670	24.570
E	MPa	5490.000	413.000	1522.000
ϕ	deg (°)	38.000	27.000	43.000
c	MPa	3.240	0.250	3.030
σ_{ci}	MPa	58.000	8.400	42.800
ν	-	0.220	0.200	0.220
m_b	-	4.680	1.200	6.940
m_i	-	20.000	8.000	20.000
S	-	0.009	0.002	0.031
a	-	0.500	0.500	0.500
D	-	0.700	0.700	0.700
GSI	-	58.000	47.000	69.000

static conditions, reflected by a critical SRF of 8.99, 3.71 and 16.57 respectively (Figure 4a, 4b and 4c)). This high

SRF value signifies a substantial margin of safety against potential failure. Additionally, the maximum shear strain recorded at the toe of the slope of SS2 is 1.20×10^{-4} and SS3 is 6.10×10^{-4} and at the middle of the SS4 is 1.12, which is minimal for all the three-slope section, suggesting very limited deformation in those regions. These low shear strain value highlights the slope's ability to resist shear forces effectively without significant internal distortion.

Moreover, the assessment reveals that the maximum total displacement occurs at the upper surface of the slope SS2, measuring $1.12 \times 10^{-4} \mathrm{m}$ (Figure 5a), middle of the slope SS3, measuring $2.10 \times 10^{-3} \mathrm{m}$ (Figure 5b) and crown of slope SS4 measuring $2.80 \times 10^{2} \mathrm{m}$ (Figure 5c). This slight displacement indicates negligible movement or shifting, reinforcing the overall stability and structural integrity of all the slopes. The minimal strain and displacement values collectively underscore the robustness of the slope under static loading conditions.

Stability modelling using PLAXIS 2D

PLAXIS 2D uses FEM to simulate complex stress-strain relationships and evaluate slope performance under various conditions (Pawar and Joshi, 2024). It provides advanced constitutive models, including the Hoek-Brown failure criterion, allowing realistic representation of rock masses and allows for the creation of slope geometries, essential for analyzing heterogeneous rock formations. uses SRM to determine the Factor of Safety (FoS) by systematically reducing the material strength until failure occurs. The modeling results too indicated that slopes SS2, SS3, and SS4 remain structurally stable when subjected to the projected conditions, provided there are no external influences from seismic activity or water forces (Figure 6). The analysis shows that the highest total displacement is observed at three slope sections: the slope SS2 is 6.40×10^{-2} m (Figure 6a), the slope SS3 is 1.84×10^{-1} m (Figure 6b), and the crown of slope SS4 is 2.50×10^{-1} m (Figure 6c). This modelling also suggests the minimal displacement with negligible movement or shifting, highlighting the overall stability and structural integrity of the slopes. The FEM modeling demonstrated that slopes SS2, SS3, and SS4 are stable under static conditions, with high SRF and minimal shear strain and displacement values, indicating strong structural integrity. The results suggest that the slopes can withstand current static loads without significant deformation, which is crucial for infrastructure planning and hazard mitigation in the region. However, the study's limitations include the exclusion of dynamic factors such as seismic activity and water pressure, which could significantly impact slope stability. Future research should incorporate these factors to provide a more comprehensive stability assessment. Additionally, long-term monitoring and periodic reassessment are recommended to account for potential changes in geological conditions and external influences, ensuring the continued safety and stability of the slopes.

Comparison of Phase2 and PLAXIS 2D results

Both analyses offer different features and ways of modeling rock slopes. The models were set up by defining the slope's shape, boundary conditions, and material properties, using the Hoek-Brown failure rule to describe the materials. Simulations were done under static conditions using the SRM to check slope stability by gradually weakening the material until it failed. The results showed that all the slopes (SS2, SS3, and SS4) stayed stable without seismic activity or water forces (Table 6). Both models confirmed the slopes were structurally strong, with little deformation at key points, meaning there was almost no movement. Although PLAXIS 2D recorded slightly higher displacement values than Phase2, both models agreed the slopes were stable and strong. Phase2 gave more detailed results, including safety factors and shear strain values, while PLAXIS 2D focused on overall slope performance through stress-strain analysis.

Table 6. Critical SRF from FEM for different slopes

Slopes	Criti	Critical SRF		
	Phase2	Plaxis 2D		
SS2	8.99	10.36		
SS3	16.57	17.31		
SS4	3.71	4.25		

The high SRF values, minimal shear strain, and negligible displacement all support that the slopes can handle static loads well.

5. Conclusions

This study evaluated the stability of critical rock slopes along the section of NH43 using kinematic analysis and FEM modeling. The results indicate that slopes SS2, SS3, and SS4 exhibit potential instability, but FEM confirmed their stability under static conditions. Specifically, the SRF values for SS2, SS3, and SS4 ranged from 3.71 to 16.57 in Phase2 and 4.25 to 17.31 in PLAXIS 2D, reflecting a substantial margin of safety against potential failure. These findings provide valuable insights for infrastructure planning in landslide-prone regions, ensuring safer road networks. However, the study did not incorporate dynamic factors such as seismic activity and water pressure, which may influence slope stability. Future research should integrate seismic loading and hydrological influences for a more comprehensive stability assessment. Additionally, long-term monitoring is recommended to assess potential

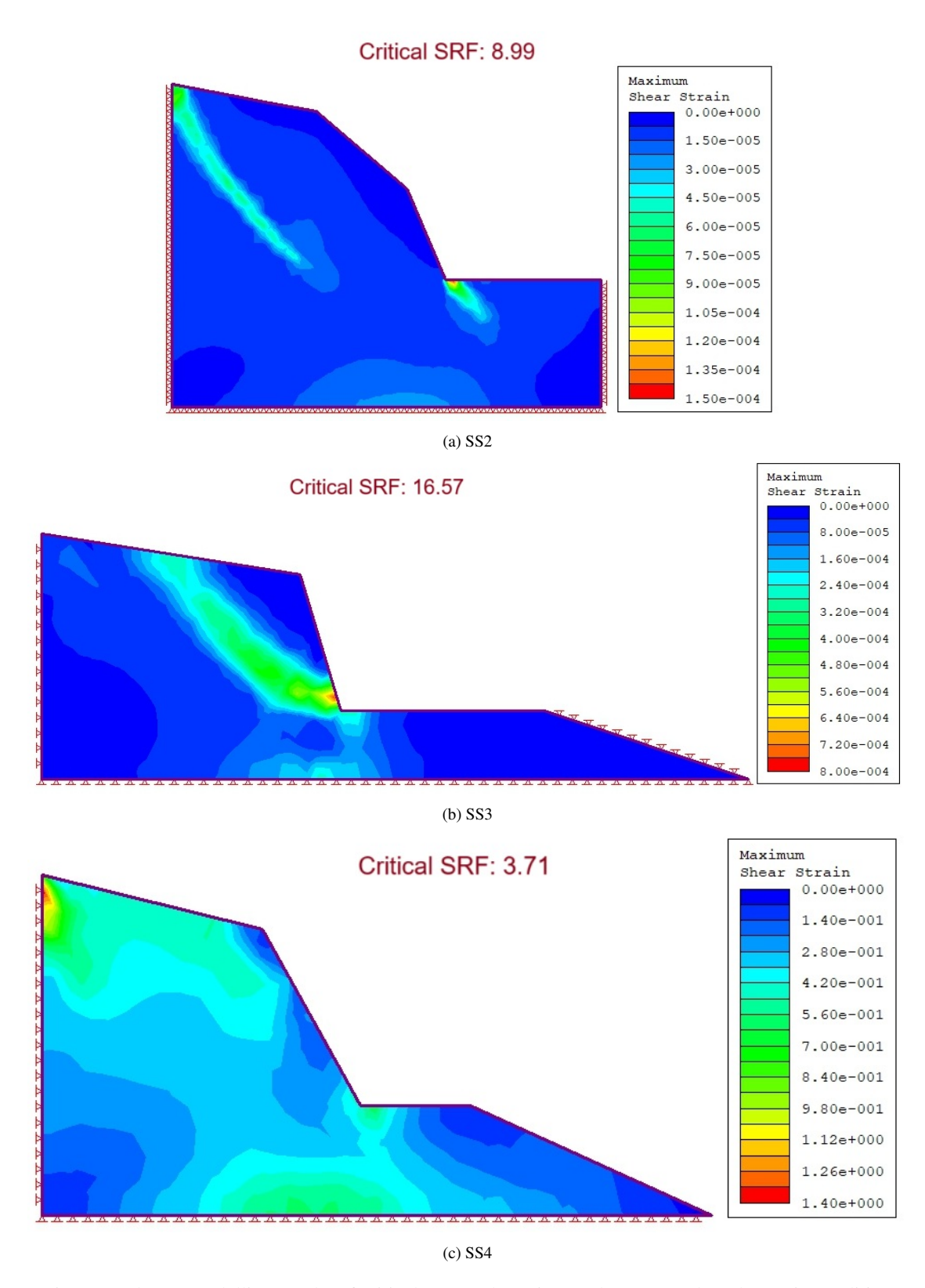


Figure 4. Phase2 modelling results of critical SRF and maximum shear strength under static condition

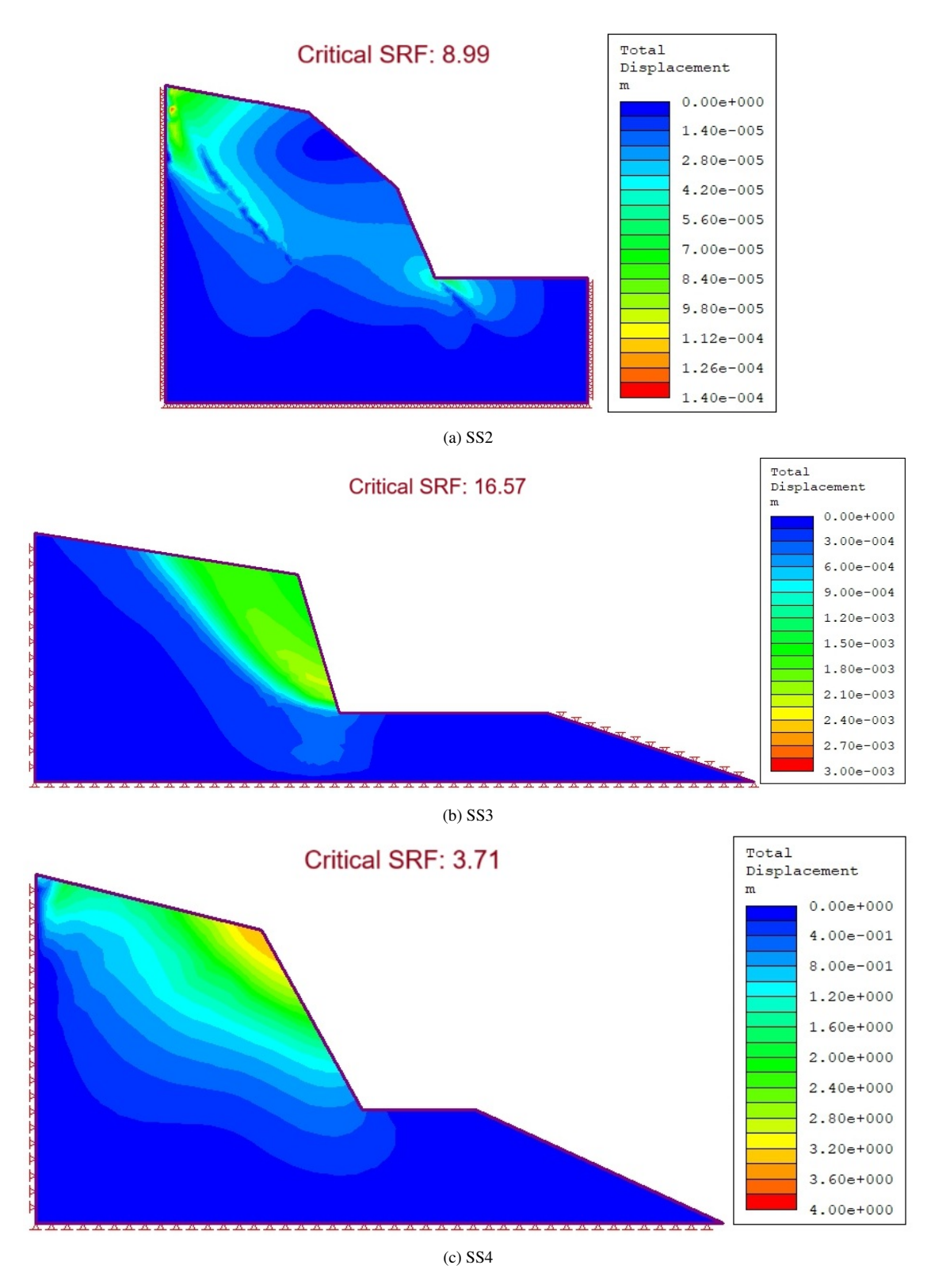
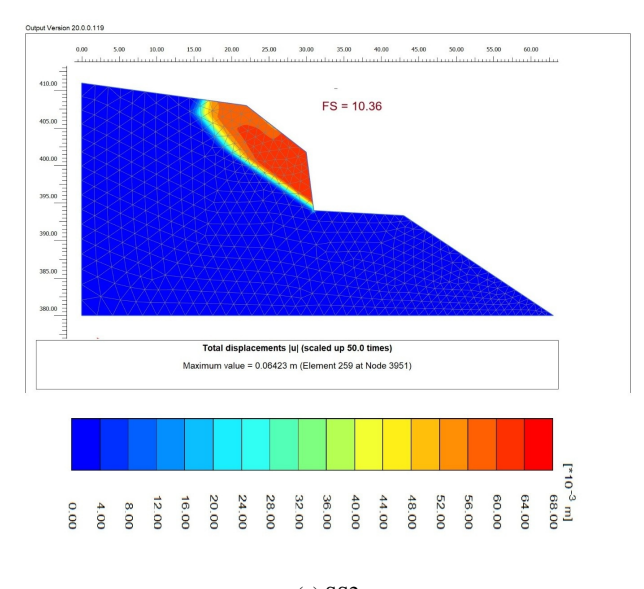


Figure 5. Phase2 modelling results of total displacement under static condition



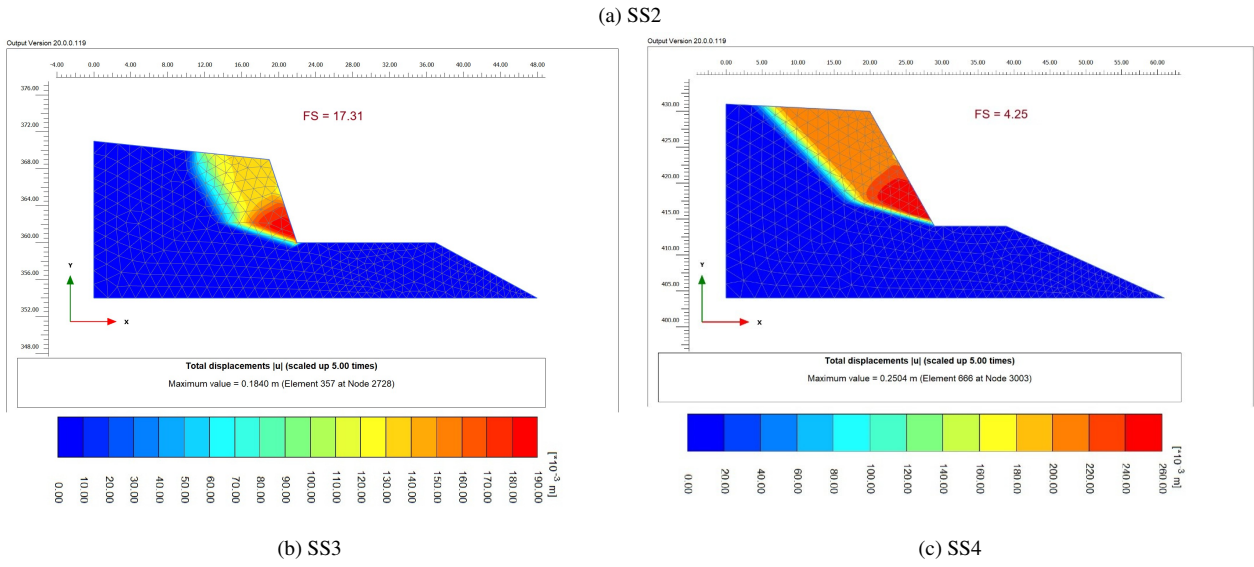


Figure 6. PLAXIS 2D modelling results of SRF and total displacement under static condition

changes over time. By incorporating continuous monitoring and further analysis, these findings can contribute to sustainable slope management and infrastructure resilience.

6. Acknowledgment

The authors extend their sincere appreciation to the anonymous reviewers for their meaningful comments, which significantly contributed to shaping the manuscript. We are also grateful to the R&D unit of Khwopa College of Engineering for providing the necessary arrangements for this study. Special thanks are given to Er. Sunil Duwal, Dr. Chandra Kiran Kawan, Dr. Raju Bhai Tyata, and Dr. Subeg Man Bijukchhen for their continuous support and encouragement throughout the research process. This study was

conducted with financial support from the Small-Scale Research Grant Program of Khwopa College of Engineering.

References

Cala, M., & Flisiak, J. (2020). Slope stability analysis with flac and limit equilibrium methods. In *Flac and numerical modeling in geomechanics-2001* (pp. 111–114). CRC Press.

Cruden, D. M., & Hu, X. Q. (1993). Exhaustion and steady state models for predicting landslide hazards in the canadian rocky mountains. *Geomorphology*, 8(4), 279–285. https://doi.org/10.1016/0169-555X(93) 90024-V

- de Freitas, M. H. (2009). Geology; its principles, practice and potential for geotechnics. *Quarterly Journal of Engineering Geology and Hydrogeology*, 42(4), 397–441. https://doi.org/10.1144/1470-9236/09-014
- DMG. (2023). Geological Map of Nepal (2nd ed.) (R. P. Ghimire, Ed.) [After modification of the first edition (1994) compiled by K. M. Amatya and B. M. Jnawali, with contributions by P. L. Shrestha, N. D. Maske, and P. Hoppe.].
- DoR. (2021). Statistics of National Highway, SHN 2020/21, Department of Road, Government of Nepal (tech. rep.).
- Fidan, S., Tanyaş, H., Akbaş, A., Lombardo, L., Petley, D. N., & Görüm, T. (2024). Understanding fatal landslides at global scales: A summary of topographic, climatic, and anthropogenic perspectives. *Natural Hazards*, *120*(7), 6437–6455. https://doi.org/10.1007/s11069-024-06487-3
- Griffiths, D. V., & Fenton, G. A. (2004). Probabilistic slope stability analysis by finite elements. *Journal of Geotechnical and Geoenvironmental Engineering*, 130(5), 507–518. https://doi.org/10.1061/(ASCE) 1090-0241(2004)130:5(507)
- Habtamu, M., Garo, T., & Chemeda, Y. C. (2022). Astu engineering geological investigation of jimma town for engineering practice. *Ethiopian Journal of Science and Sustainable Development*, 9(1). https://doi.org/10.20372/ejssdastu:v9.i1.2022.400
- Hoek, E., & Brown, E. T. (1997). Practical estimates of rock mass strength. *International Journal of Rock Mechanics and Mining Sciences*, 34(8), 1165–1186. https://doi.org/10.1016/S1365-1609(97)80069-X
- Hoek, E., Carranza-Torres, C., & Corkum, B. (2002). *Hoek-brown failure criterion-2002 edition* (tech. rep.). Rocscience. www.rocscience.com
- Hoek, E., & Kaiser, P. K. (1995). Support of underground excavation in hard rock. ResearchGate. https://www.researchgate.net/publication/37408005
- Hoek, E., & Marinos, P. (2007). A brief history of the development of the hoek-brown failure criterion. *Rock Mechanics and Rock Engineering*.
- ISRM. (1979). Suggested methods for the quantitative description of discontinuities in rock masses. *International Journal of Rock Mechanics and Mining Sciences & Geomechanics Abstracts*, *16*(2), 22. https://doi.org/10.1016/0148-9062(79)91476-1
- Park, H. J., Lee, J. H., Kim, K. M., & Um, J. G. (2016). Assessment of rock slope stability using gis-based probabilistic kinematic analysis. *Engineering Geology*, 203, 56–69. https://doi.org/10.1016/j.enggeo.2015.08.021

- Pawar, H. M., & Joshi, S. R. (2024). Analysis of slope stability and landslide by using plaxis 2d. *Research Journal of Science and Technology*, *16*(1), 29–38. https://doi.org/10.52711/2349-2988.2024.00006
- Rechberger, C., Fey, C., & Zangerl, C. (2021). Structural characterisation, internal deformation, and kinematics of an active deep-seated rock slide in a valley glacier retreat area. *Engineering Geology*, 286, 106048. https://doi.org/10.1016/j.enggeo.2021. 106048
- Rocscience. (2015). *Phase2 version 8.0, finite element analysis for excavations and slopes.*
- Rocscience. (2016). Dips version 7.0, graphical and statistical analysis of orientation data.
- Stöcklin, J. (1980). Geology of Nepal and its regional frame. *Journal of the Geological Society*, *137*(1), 1–34. https://doi.org/10.1144/gsigs.137.1.0001
- Vásárhelyi, B. (2009). A possible method for estimating the poisson's rate values of the rock masses. *Acta Geodaetica et Geophysica Hungarica*, 44(3), 313–322. https://doi.org/10.1556/AGeod.44.2009.3.4
- Wyllie, D. C., & Mah, C. W. (2017). *Rock slope engineering*. CRC Press. https://doi.org/10.1201/9781315274980

This work is licensed under a Creative Commons "Attribution-NonCommercial-NoDerivatives 4.0 International" license.

